ELSEVIER

Catalysis Today 62 (2000) 367–377

CATALYSIS TODAY

www.elsevier.com/locate/cattod

Performance of zeolites and product selectivity in the gas-phase oxidation of 1,2-dichloroethane

R. López-Fonseca, A. Aranzabal, P. Steltenpohl[1], J.I. Gutiérrez-Ortiz, J.R. González-Velasco*

Department of Chemical Engineering, Faculty of Sciences, University of the Basque Country/EHU, P.O. Box 644, E-48080 Bilbao, Spain

Abstract

The deep oxidation of 1,2-dichloroethane (DCE) over H-type zeolites (H-Y, H-ZSM-5 and H-MOR) was evaluated. Experiments were performed on conditions of lean chlorocarbon concentration (around 1000 ppmv) under dry and humid conditions, between 200 and 550°C in a conventional fixed-bed reactor. The high density of Brønsted acid sites, proved by temperature-programmed desorption (TPD) of ammonia and diffuse reflectance FT-IR of adsorbed pyridine measurements, make H-ZSM-5 zeolite an effective catalyst for DCE decomposition. Vinyl chloride was identified as an intermediate in 250–400°C range. When vinyl chloride was destroyed at higher temperatures, all the zeolites showed a great selectivity (>90%) to HCl. CO was promoted in quantity reflecting the difficulty of its oxidation over these zeolite catalysts. The activity of the zeolites was reduced in the presence of water vapour (15,000 ppmv). It was noticed that the addition of water to the feed stream did not alter the order of activity observed in the dry experiments. Moreover, the presence of water in the DCE decomposition changed significantly the reaction product distribution. Vinyl chloride formation was found to be significantly lowered over the three zeolites, and selectivity to CO_2 formation was largely enhanced. The X-ray powder diffraction (XRD) analysis of the deactivated samples indicated partial destruction of the zeolite crystal structure during reaction.

Keywords: Catalytic oxidation; Chlorinated volatile organic compounds; 1,2-Dichloroethane; H-type zeolites; H-Y; H-ZSM-5; H-MOR; Brønsted acidity; Selectivity

1. Introduction

Chlorinated volatile organic compounds (CVOCs) are emitted to the atmosphere in flue gases from a variety of industrial processes. Chlorinated hydrocarbons have enjoyed widespread acceptance as solvents in the chemical industry because of their relative inertness in chemical processes and their ability to dissolve many organic compounds. Chlororganics are among the most widespread and persistent toxic pollutants which are hazardous to human health and the environment. Such compounds are typically carcinogens, mutagens and teratogens, and are involved in the destruction of the ozone layer as well. Hence, public awareness of the harmful effects of CVOCs emissions has led to increasingly stringent environmental regulations. The Clean Air Act Amendments of 1990 establish health based air quality standards and provide for the significant reduction of emissions. 1,2-Dichloroethane (DCE) is one of the main pollutants generated in vinyl chloride

* Corresponding author. Tel.: +34-94-6012681; fax: +34-94-4648500.
E-mail address: iqpgovej@lg.ehu.es (J.R. González-Velasco).
[1] On leave from Department of Chemical and Biochemical Engineering, Slovak University of Technology, 812 37 Bratislava, Slovak Republic.

0920-5861/00/$ – see front matter
PII: S0920-5861(00)00438-7

monomer production plants [1] and is also found in groundwater air-stripping emissions admixtured with other chlorinated solvents such as trichloroethylene, dichloromethane and 1,2-dichloroethylene [2].

In recent years, catalytic oxidation of CVOCs has become a widely adopted method of destruction and is a strongly favoured alternative in view of the potential technological and economic advantages compared to thermal incineration. The practical applications of the catalytic oxidation processes require heating large volumes of gas containing low concentrations of CVOCs to oxidation temperature (300–550°C). In addition, most of the industrial waste gases are often saturated with water vapour. This corresponds to an absolute water content between 0.8 and 3.1% in the exit stream [3].

Noble metal-based catalysts in general, exhibit the highest activity for the oxidation of volatile organic compounds. Such catalysts are not particularly suited for the destruction of CVOCs, since they undergo severe deactivation due to halide poisoning of the noble metal and are susceptible to the formation of volatile metal oxychlorides [4]. Alternatively, the use of transition metal oxides has been proposed because of their resistance to deactivation, however, their destruction activity is often lower [5]. Other types of catalysts, such as pillared clays, molten salt-based systems, perovskites, and MS41 mesoporous materials have also been considered for CVOCs control [6–9]. In last decades, zeolites have received great interest because of their optimum performances as solid acid catalysts in refining and petrochemical processes [10,11], and as adsorbents in many separation and purification processes [12], but less consideration has been given to study the applicability of zeolites for the decomposition of CVOCs [13–15]. Thus, zeolite catalysts should be considered as an effective alternative to the noble and metal oxide catalysts employed in most commercial applications.

This study investigates the suitability of zeolites for the oxidative decomposition of DCE. It focuses on H-Y, H-ZSM-5 and H-MOR zeolites, which are good candidates as catalysts in many industrial applications. The scope of this study is to compare the catalytic activity and product selectivity in the DCE oxidation of a range of H-type zeolites with varying topologies at lean chlorocarbon concentration conditions (around 1000 ppmv) under excess of air between 200 and 550°C. The effect of water addition (15,000 ppmv) to the feed stream has also been discussed.

2. Experimental

2.1. Materials and catalyst characterisation

The zeolites H-Y (CBV400), NH_4-ZSM-5 (CBV-5524G) and Na-MOR (CP500C-11) were supplied from the PQ Corp. The H-Y zeolite was used as received. The H-ZSM-5 zeolite was obtained by calcining the NH_4-ZSM-5 zeolite in air at 550°C for 3 h. The mordenite sample in the NH_4-form was prepared by two successive ion exchanges with a 3 M NH_4NO_3 solution at room temperature for 24 h. The NH_4-form was then transformed to the H-form by calcining air at 550°C for 3 h. The zeolites were pelletised using methylcellulose as a temporary binder which was removed by calcination in air. Then the pellets were crushed and sieved to grains of 0.3–0.5 mm in diameter.

The BET surface areas of the zeolite samples were determined by N_2 adsorption–desorption at −196°C in a Micromeritics ASAP 2010 equipment. The compositions were determined using a Philips PW 1480 X-ray fluorescence (XRF) spectrometer. The X-ray powder diffraction (XRD) patterns were recorded on a Philips PW 1710 X-ray diffractometer with Cu Kα radiation.

Temperature-programmed desorption (TPD) of ammonia was performed on a Micromeritics AutoChem 2910 instrument. Prior to adsorption experiments, the samples (30–40 mg) were first pre-treated in a quartz U-tube in a nitrogen stream at 500°C. Then, they were cooled down at 100°C in a N_2 flow (20 $cm^3\,min^{-1}$) before the ammonia adsorption started. The adsorption step was performed by admitting small pulses of ammonia in Ar at 100°C up to saturation. Subsequently, the samples were exposed to a flow of argon (50 $cm^3\,min^{-1}$) for 2 h at 100°C in order to remove reversibly and physically bound ammonia from the surface. Finally, the desorption was carried out from 100 to 500°C at a heating rate of 10°C per min in an Ar stream (50 $cm^3\,min^{-1}$). This temperature was maintained for 15 min until the adsorbate was completely desorbed.

Diffuse reflectance (DRIFT) spectra of pyridine adsorbed on the zeolite samples were obtained from a

Nicolet Protegé 460 ESP spectrometer, equipped with a Spectra-tech high-temperature chamber, with KBr windows and a liquid nitrogen-cooled MCT detector. All the spectra were collected in 4000–650 cm^{-1} range averaging 400 scans with a 1 cm^{-1} resolution and analysed using OMNIC software. After the sample was evacuated at 500°C and 10^{-5} Torr (1 Torr = 133.3 N m^{-2}) for 1 h, pyridine vapour was admitted in doses at 200°C until the catalyst surface was saturated. Pyridine was desorbed until a pressure of 10^{-5} Torr to ensure that there was no more physisorbed pyridine. The spectra of adsorbed pyridine were then measured. Difference spectra were obtained by subtracting the spectrum of the dehydrated zeolite sample from the spectra obtained after pyridine adsorption.

2.2. Catalytic activity measurement

Oxidation reactions were carried out in a conventional fixed-bed reactor under atmospheric pressure. It consisted of 12 mm i.d. stainless steel tube located inside an electrical furnace. At the lower part of the reactor, 0.85 g (around 2 cm^3) of catalyst was placed on a plug of glass wool. In order to preheat the gas feed stream crushed quartz glass (10 cm^3, 2 mm o.d.) was placed above the catalyst bed. The temperature was measured automatically with a K-type thermocouple.

The flow rate through the reactor was set at 500 cm^3 min^{-1} and the gas hourly space velocity (GHSV) was maintained at 15,000 h^{-1}. The feed stream to the reactor was prepared by delivering the liquid chlorinated hydrocarbon (1000 ppmv of DCE) and water (15,000 ppmv) by two syringe pumps into a dry, oil-free compressed air, which was purified using a commercial PSA drier and metered by a mass flow controller. The injection points were electrically heated to ensure complete evaporation of both reactants. Before entering the reactor, the feed stream went through a 2 cm^3 static mixer to dampen out possible concentration oscillations associated with the running of the syringe pumps. Teflon tubing was employed due to its inertness and insensitivity to corrosion by hydrogen chloride. Negligible corrosion of the stainless steel reactor was expected above 200°C [16]. Subsequently, the temperature was raised from 200 to 550°C in steps of 50°C, and after a stabilisation of 10 min, effluent gases were analysed.

A portion of the effluent stream was analysed on line by a Hewlett Packard 5890 Series II gas chromatograph equipped with an electron capture detector (ECD) and a thermal conductivity detector (TCD). CO and CO_2 were separated both by a 13X molecular sieve column and a Hayesep N column interconnected to a gas sampling loop by a single 10-port valve and were analysed using the TCD. The concentration of either DCE and any other chlorinated hydrocarbons formed in the reaction were determined by the ECD after being separated in a HP-VOC column. Analysis of both Cl_2 and HCl was performed by bubbling the effluent stream through a 0.0125 N NaOH solution [17]. The Cl_2 concentration was determined by titration with ferrous ammonium sulphate (FAS) using *N*,*N*-diethyl-*p*-phenylenediamine (DPD) as an indicator [18]. The concentration of chloride ions in the bubbled solution was determined by using an ion selective electrode.

3. Results and discussion

3.1. Catalyst characterisation

The compositions, Si/Al atomic ratios and BET areas for H-type zeolites tested in this study are given in Table 1. The water content was determined as the percentage difference between the weight of water satured samples and calcined ones at 900°C.

TPD of ammonia and infrared (IR) of adsorbed pyridine are probably the most extensively used methods for characterising acidity in zeolites [19]. The amount of ammonia desorbed at relatively low temperature is taken as a measure of the acid sites concentration while the temperature range in which most of ammonia is desorbed indicates the acid-strength distribution. IR spectroscopy of adsorbed pyridine mainly shows the nature of the acid sites, discriminating between Brønsted and Lewis sites.

Fig. 1 shows the diffuse-reflectance IR spectra of pyridine adsorbed on the zeolites at 200°C in the region 1700–1400 cm^{-1} at 10^{-5} Torr. All the samples exhibited bands due to hydrogen bonded pyridine (1596 cm^{-1}), Lewis bound pyridine (1623, 1575 and 1455 cm^{-1}), pyridinium ion ring vibration due to pyridine bound to Brønsted acid sites (1545 and 1639 cm^{-1}) and a band at 1492 cm^{-1} which can be assigned to pyridine associated with Brønsted and Lewis

Table 1
Physicochemical properties of the zeolite catalysts

	SiO_2 (%)	Al_2O_3 (%)	Na_2O (%)	H_2O (%)	Si/Al	S_{BET} ($m^2\,g^{-1}$)
H-Y	73.5	23.7	2.7	12.3	2.4	730
H-ZSM-5	97.1	2.8	0.1	7.2	27.3	425
H-MOR	91.0	8.8	0.2	5.2	5.2	400

sites [20,21]. In the literature, the bands at 1545 and 1455 cm^{-1} are used for the determination of Brønsted and Lewis sites, respectively [22,23]. All the samples contained both Brønsted and Lewis acidity. H-Y possesses a large number of both types of acid sites with a ratio of Brønsted to Lewis acid sites, measured as the ratio of the integrated areas of the respective pyridine bands, equal to 0.8. On the other hand, H-ZSM-5 and H-MOR contain predominantly Brønsted sites, since the absorption band at 1455 cm^{-1} attributed to pyridine bonded to Lewis sites was very low [24,25].

The results from NH_3-TPD experiments are plotted in Fig. 2. The NH_3 described above 100°C was considered as chemisorbed NH_3 and subsequently used for acidity determination. The order according to their overall acidity resulted to be: H-MOR > H-Y > H-ZSM-5 (Table 2). The position of the temperature maximum of the ammonia desorption versus temperature graph is a qualitative indication of the magnitude of the NH_3 desorption activation energy and consequently the relative acid strength of the sites [26]. As can be seen in these graphs, all the curves displayed a major desorption peak around 150°C. This peak is indicative of the weak (Brønsted and/or Lewis) sites present in the zeolite catalysts. Apart from the temperature maximum of the NH_3 desorption curve, the area under this desorption peak is also indicative of the relative number of acid sites present. Comparing the desorption curves of the different catalysts, it is found that the apparent number of weak sites was similar in H-Y and H-MOR (around 50% of the total acid sites) and larger than in H-ZSM-5 (about 40%).

A second much smaller desorption peak was obtained for H-ZSM-5 and H-MOR samples in 350–450°C range, indicating the presence of strong Brønsted acid sites. On the contrary, H-Y showed almost no inflection in this region. According to the DRIFT measurements of adsorbed pyridine at 300°C, the Brønsted/Lewis acid sites ratio in H-Y zeolite was

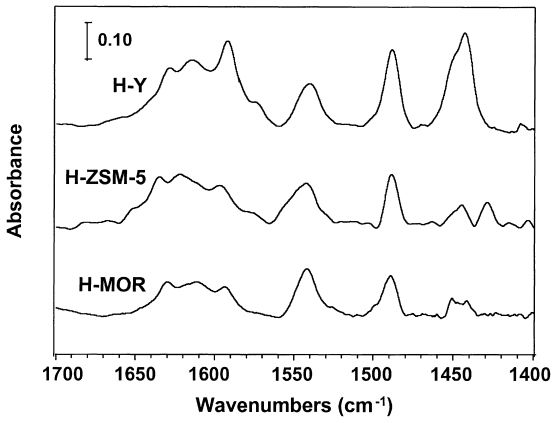

Fig. 1. Diffuse-reflectance IR spectra of pyridine adsorbed on H-Y, H-ZSM-5 and H-MOR zeolites.

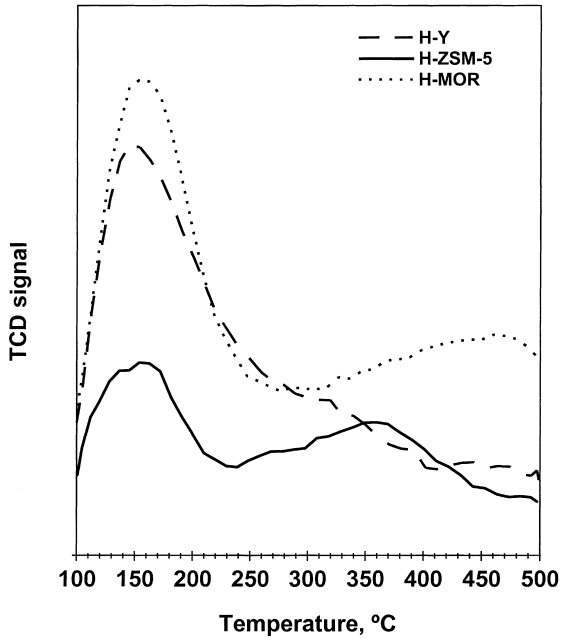

Fig. 2. TPD of ammonia spectra from H-Y, H-ZSM-5 and H-MOR zeolites.

Table 2
Total acidity and density of acid sites of the H-type zeolites

Zeolite	Total acidity (mmol $NH_3\,g^{-1}$)	NH_3 (%) desorbed at different temperatures							
		150°C	200°C	250°C	300°C	350°C	400°C	450°C	500°C
H-Y	0.651	20.8	32.6	46.9	55.8	63.4	77.0	89.2	98.6
H-ZSM-5	0.489	13.5	27.1	40.8	50.1	61.2	72.4	85.4	98.2
H-MOR	0.972	19.6	34.8	48.8	60.0	68.2	78.8	87.3	98.1

1.1 and the number of strong Brønsted sites therefore resulted $0.149\,mmol\,g^{-1}$ compared with 0.244 and $0.689\,mmol\,g^{-1}$ in H-ZSM-5 and H-MOR, respectively. On the other hand, it could be concluded from Table 2 that the density of strong Brønsted sites in H-ZSM-5 resulted higher than that in H-MOR. Furthermore, it has been reported that about 2/3 of the acid sites in H-MOR zeolite are located in the large channels and are accessible to larger organic compounds such as DCE (5.2 Å), whereas about 1/3 of them are in the narrow channels and are accessible only to small molecules such as ammonia [27–29]. Accordingly, they are considered to be inactive sites and the relative population of active sites is therefore reduced significantly.

3.2. Activity tests

The oxidation activity is best illustrated by showing the evolution of conversion with temperature, namely, the light-off curve. Fig. 3 shows the light-off curves for DCE oxidation over H-Y, H-ZSM-5 and H-MOR zeolite catalysts, and without any catalyst. The latter was performed placing just 0.3–0.5 mm quartz glass into the reactor.

Fig. 3 shows that thermal oxidation occurred only above 425°C. Kiebling et al. [30] also reported homogeneous gas oxidation of DCE at temperatures above 400°C. The studied H-type zeolites exhibited high activity in the oxidative decomposition of DCE. It was found that the order of activity was: H-ZSM-5 > H-MOR > H–Y. H-ZSM-5 showed a T_{50} (temperature at which 50% conversion is achieved) of 275°C compared with 290 and 325°C obtained by H-MOR and H-Y zeolites, respectively. The complete oxidation was attained above 350°C with H-ZSM-5 and above 400°C with H-MOR and H-Y. Hence, the use of H-type zeolites as catalysts advances the destruction temperatures about 200°C in comparison to the thermal decomposition of DCE. Nagata et al. [31] reported high activity of H-type zeolites in the decomposition of chlorofluorocarbons. Likewise, Tajima et al. [32] examined several solid acid catalysts for the decomposition of cholorofluorocarbons and reported that the H-type zeolites showed the highest destruction activity. Similarly, Greene et al. [33] and González-Velasco et al. [34] found H-ZSM-5 zeolite more reactive than H-Y zeolite in the oxidation of carbon tetrachloride and trichloroethylene, respectively.

It is well accepted in the literature that Brønsted acidity plays a key role in determining the activity of acidic catalysts since the oxidation of chlorinated

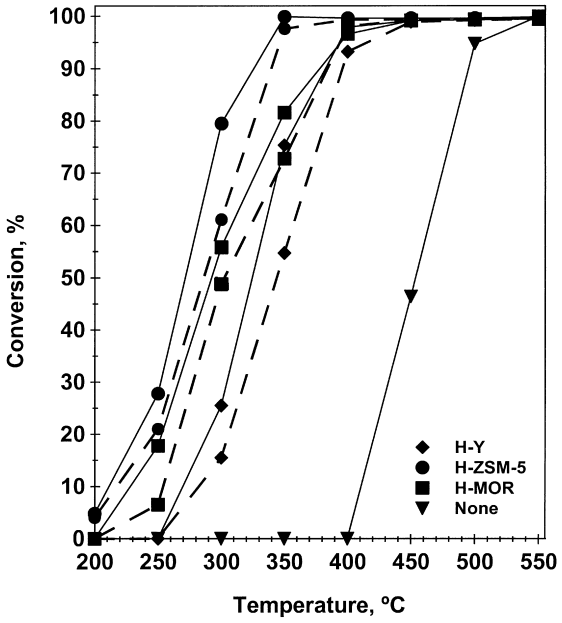

Fig. 3. DCE oxidation light-off curves over H-Y, H-ZSM-5 and H-MOR zeolites, and empty reactor (homogeneous reaction) under dry conditions (—) and humid conditions (– – – –).

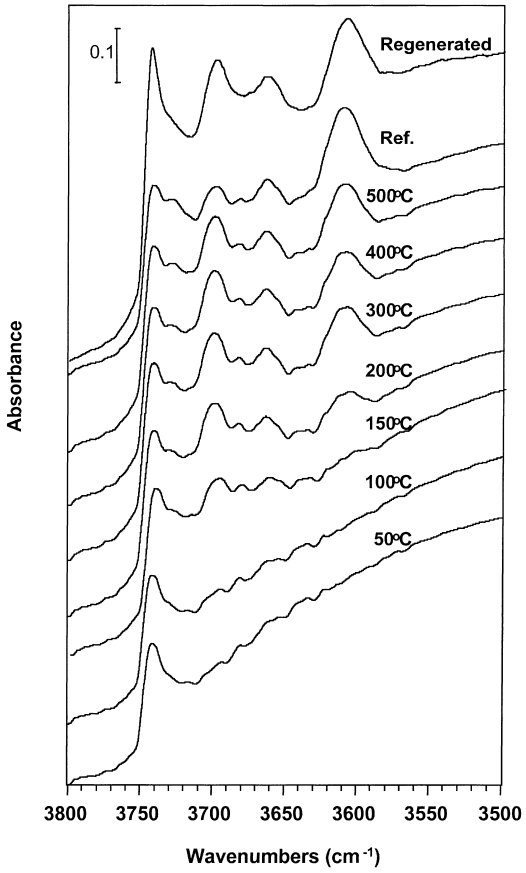

Fig. 4. DRIFT spectra of DCE adsorbed on H-ZSM-5 zeolite at different temperatures and DRIFT spectrum of the regenerated H-ZSM-5 sample.

hydrocarbons is initiated by the adsorption of the hydrocarbons on these sites [6,15,32,35]. In order to obtain insights on the surface phenomena in the reaction process, DCE adsorption on H-ZSM-5 zeolite sample was analysed by means of in situ DRIFT spectroscopy. The IR spectra of the zeolite hydroxyls are shown in Fig. 4 during DCE adsorption at different temperatures. In the spectrum of the H-ZSM-5 sample pre-treated at 500°C in vacuum, two absorption bands were observed at 3740 cm^{-1} attributed to non-acidic terminal silanols and at 3609 cm^{-1} assigned to Brønsted acid sites, i.e. a hydroxyl group bridging between silicon and aluminium within the zeolite pores. An additional small absorption band was detected at 3670 cm^{-1} which was associated with AlOH groups involving partially extra framework alumina species [36]. By admitting DCE onto the sample, the band at 3609 cm^{-1} completely disappeared while the band at 3740 cm^{-1} remained intact. This interaction was studied by following the restoration of the band at 3609 cm^{-1} upon desorbing DCE in vacuum at increasing temperatures. The results showed that the IR band was recovered only after heating at about 300°C. This behaviour clearly indicated that Brønsted acid sites acted as effective chemisorption sites for DCE. No complete restoration of the band was noticed due to the coverage of the acid sites by the coke formed at high temperatures [37]. Afterwards, coke was completely burnt off at 550°C in air leading to the restoration of the full intensity of the absorption band (Fig. 4). This proved that the H-ZSM-5 zeolite could be completely regenerated through an oxidative treatment.

3.3. Product distribution of DCE decomposition

Figs. 5 and 6 show the product distribution versus reaction temperature when DCE was decomposed under air-rich conditions with H-type zeolite cata-

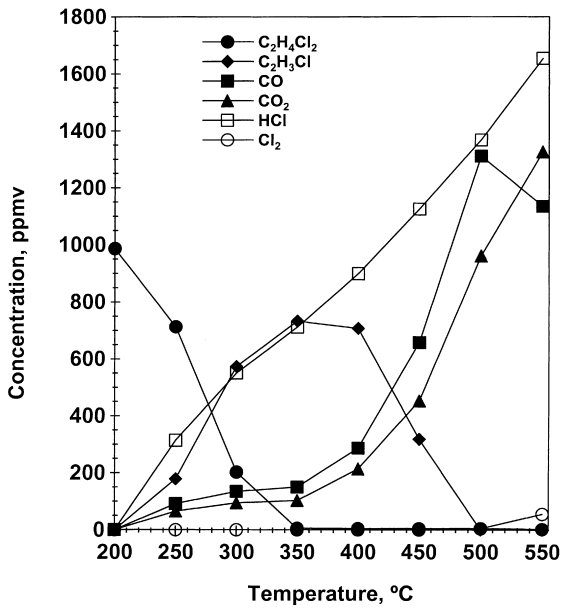

Fig. 5. Concentration profiles of reactant and products at various temperatures in the DCE oxidation over H-ZSM-5 zeolite under dry conditions.

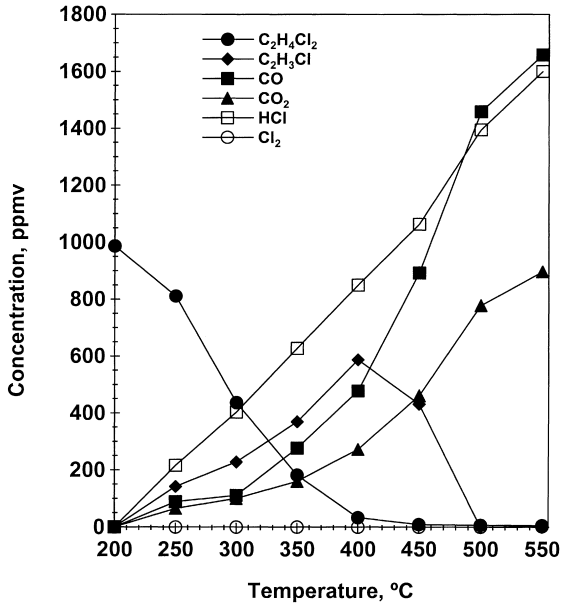

Fig. 6. Concentration profiles of reactant and products at various temperatures in the DCE oxidation over H-MOR zeolite under dry conditions.

lysts. DCE was completely converted at 350°C using H-ZSM-5 zeolite, whereas full conversion was achieved at 400°C with H-MOR and H-Y zeolites. The main oxidation products were vinyl chloride, carbon monoxide, carbon dioxide and hydrogen chloride.

Amounts of vinyl chloride were detected at 250°C when DCE first started to react. The vinyl chloride concentration passed through a maximum at 350°C for H-ZSM-5 zeolite and at 400°C for H-MOR and H-Y zeolites. The presence of this intermediate suggests that the abstraction of HCl (dehydrochlorination) is the first step in the reaction process. The peak concentrations of vinyl chloride were 860, 735 and 590 ppmv for H-Y, H-ZSM-5 and H-MOR, respectively. Vinyl chloride, being stable, did not undergo further dehydrochlorination, and oxidised to CO, CO_2 and HCl at higher temperatures. Further evidence of the HCl abstraction mechanism has been found by Ramanathan and Spivey [38] and Windawi and Wyatt [39] in the oxidation of 1,1,1-trichloroethane, where 1,1-dichloroethylene was identified as an intermediate. Ranging from 250 to 400°C, the relation between the decline of DCE and the rise of vinyl chloride and HCl was almost linear. Also, the maximum concentration for vinyl chloride occurred at the temperature when DCE was completely consumed, i.e. an additional indication that this intermediate was directly formed from DCE. Neither CO nor CO_2 appeared to be formed to any appreciable extent until vinyl chloride decomposition started at about 350°C in the case of H-ZSM-5 and 400°C in the case of H-MOR and H-Y zeolites. Trace amounts of HCl, CO and CO_2 were measured at low temperatures as a result of direct DCE oxidation. No phosgene ($COCl_2$) was detected in the product stream of any catalyst. This absence was confirmed by the use of detector tubes (dräger tubes).

Some other partial oxidation products were formed, namely chloroform ($CHCl_3$), trichloroacetaldehyde (C_2Cl_3HO), trichloroethylene (C_2HCl_3) and tetrachloroethylene (C_2Cl_4) at the lower temperature range, but their concentration was always below 20 ppmv. These by-products were completely decomposed at 450°C. Chloroform is a cracking product while trichloroethylene and tetrachloroethylene are formed by dehydrochlorination of the DCE followed by chlorination. The formation of trichloroacetaldehyde can be explained by oxychlorination of the DCE with oxygen and HCl. Lago et al. [7] examined $CuCl/KCl/SiO_2$ as catalyst for the oxidation of DCE. At temperatures below 450°C, the chloride catalyst activated H–Cl exchange and trichloroethane, tetrachloroethane and dichloroethylene were produced. Schneider et al. [8] also detected the formation of higher chlorinated hydrocarbons in the oxidation of DCE using a $LaMnO_3$ perovskite type catalyst.

The following reaction pathway may be postulated based on the experimental data observation.

$$C_2H_4Cl_2 \rightarrow C_2H_3Cl + HCl \quad (1)$$

$$C_2H_3Cl + (\tfrac{1}{2} + x)O_2 \rightarrow 2CO_x + HCl + H_2O$$
$$x = 1, 2 \quad (2)$$

which sum up to

$$C_2H_4Cl_2 + (\tfrac{1}{2} + x)O_2 \rightarrow 2CO_x + 2HCl + H_2O$$
$$x = 1, 2 \quad (3)$$

In addition, trace amounts of chlorine were also produced by the Deacon reaction.

$$2HCl + \tfrac{1}{2}O_2 \leftrightarrow Cl_2 + H_2O \quad (4)$$

Reaction (4) did not take place appreciably except at temperatures above 500°C and even a maximum of only 60 ppmv of chlorine was detected at these temperatures. The production of Cl_2 is not environmentally desirable. In contrast, HCl is less toxic and can be easily trapped and neutralised from the effluent gas stream with a caustic solution and discarded as brine, thereby reducing corrosion problems in downstream processing equipment. DCE is commonly used as a model compound, because it contains enough hydrogen atoms in the molecule itself and is suitable to analyse the selectivity of a given catalyst towards HCl generation. H-type zeolites are poor Deacon catalysts in comparison to metals which are extremely active for this reaction leading to the formation of undesired chlorine [40–43]. When vinyl chloride was destroyed at higher temperatures, zeolite catalysts showed a high selectivity (>90%) towards HCl formation.

The selectivity values towards CO and CO_2 are calculated as follows

$$S_{CO} = \frac{CO}{CO + CO_2} \times 100 \quad (5)$$

$$S_{CO_2} = \frac{CO_2}{CO + CO_2} \times 100 \quad (6)$$

resulting selectivity values around 35% over H-MOR, whereas H-Y and H-ZSM-5 were found to be slightly more selective (40%) to CO_2 formation. CO oxidation to CO_2 was only observed at 550°C with H-ZSM-5, where selectivity to CO_2 around 60% was obtained. The formation of carbon monoxide over H-type zeolites reflects the difficulty of its oxidation over these catalysts. Jiang et al. [44] found that CO was favoured in the oxidation of methylene chloride over acidic sulphated oxide catalysts. Similarly, van der Brink et al. [45,46] reported that CO was the predominant deep oxidation product during the decomposition of several chlorocarbons over γ-alumina.

3.4. Influence of water on catalytic activity and product distribution

Fig. 3 shows the light-off curves of the DCE oxidation carried out under humid conditions. It was noticed that the addition of water (15,000 ppmv) to the feed stream did not alter the order of activity observed in the dry experiments. The activity of the zeolites was reduced in the presence of water vapour. Hence, T_{50} values increased from 275 to 285°C over H-ZSM-5, from 290 to 305°C over H-MOR, and from 325 to 350°C over H-Y. It has been reported in the literature [9,33,46–49] that CVOC destruction activity of various catalysts is generally decreased upon contacting with a high concentration of water vapour. This inhibition by water probably reflects the competition of the reactant molecules with water molecules for adsorption on the active sites.

The effect of water presence on the activity of H-Y zeolite resulted in a noticeable decrease in the DCE conversion, as the complete destruction required 450°C compared with 400°C in the absence of water. On the contrary, the addition of water in the feed stream had a minimal effect on the conversion of H-ZSM-5 and H-MOR zeolites. The drop in activity of H-Y is associated with the strong hydrophilic character of aluminium-rich zeolites such as H-Y. This is in stark contrast with zeolites with high Si/Al ratio such as H-ZSM-5, which are markedly hydrophobic, and therefore offer reduced sensibility to water inhibition of active sites [50,51].

Moreover, the presence of water in the DCE decomposition changed markedly the reaction product distribution (Figs. 7 and 8). Vinyl chloride formation was found to be significantly reduced over the three zeolites. The inhibiting effect of water on the formation of reaction intermediates was consistent with previous reports on the oxidation of 1,1,1-trichloroethane [39] and dichloromethane [45]. In the runs over H-Y and H-ZSM-5 vinyl chloride production was half of that produced under dry conditions, whereas the amount of vinyl chloride was decreased by a factor of 4 over H-MOR. In addition, the formation of chlorinated by-products, i.e. $CHCl_3$, C_2Cl_3HO, C_2HCl_3 and C_2Cl_4, was completely suppressed. Water also promoted the oxidation of CO [52], by the water-shift reaction, and as a result selectivity to CO_2 at 550°C was around 60, 70 and 80% over H-Y, H-ZSM-5 and H-MOR, respectively. Likewise, the excess of water led to complete reaction of chlorine to HCl resulting in 100% selectivity values in all the cases.

Carbon balance in the catalytic runs conducted under dry conditions was within 80–90% from 200 to 450°C. Furthermore, the catalysts became darker, which indicated deposition of carbonaceous material [13,53,54]. It should also be pointed out that the

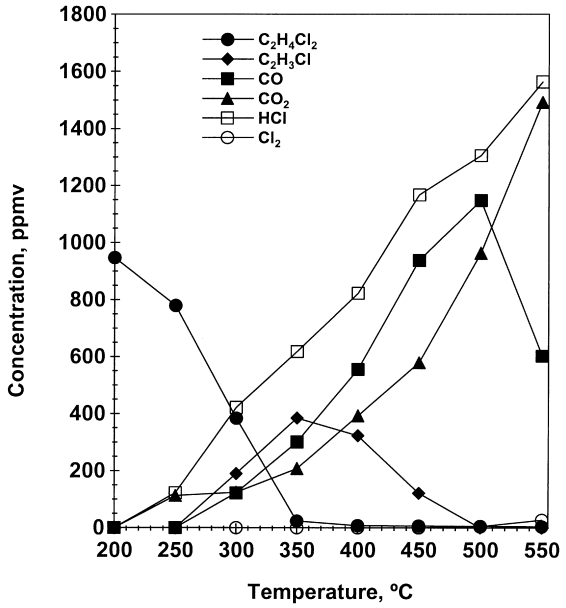

Fig. 7. Concentration profiles of reactant and products at various temperatures in the DCE oxidation over H-ZSM-5 zeolite under humid conditions.

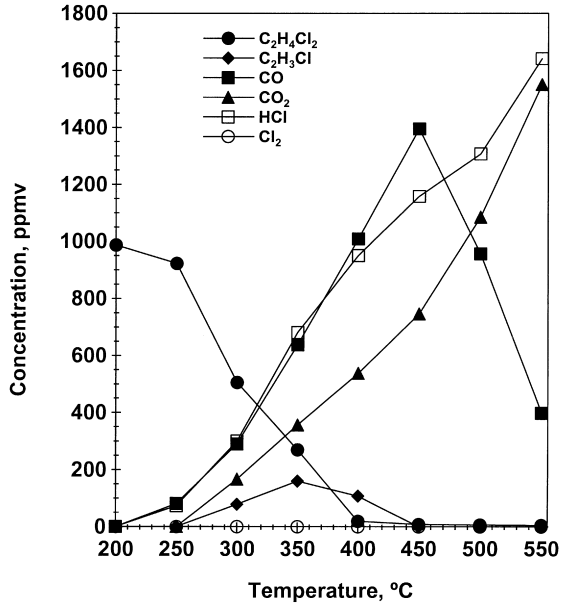

Fig. 8. Concentration profiles of reactant and products at various temperatures in the DCE oxidation over H-MOR zeolite under humid conditions.

carbon balances were found to be higher than 100% at elevated temperatures due to the combustion of the coke formed during reaction, which lasted about 8 h. Deactivation of a zeolite catalyst by coking is a process that strongly depends on the zeolite pore size and inter-connectivity of channels [37,53]. When the pore system is constituted of non-connecting channels as in H-MOR, deactivation occurs through pore blockage. Active sites in H-MOR are only accessible through these unidirectional channels and blockage by coking of a channel leading to active sites completely hinders the access to those sites. Coke has therefore a great deactivating effect in this type of zeolites. This would provide an additional evidence in order to explain the low activity of H-MOR in DCE conversion. Conversely, in the case of zeolites such as ZSM-5, interconnected channel system offers multiple paths to the active sites and thus coke has a moderate deactivating effect. Nevertheless, under humid conditions carbon balance resulted to be within 90–100%, noting that no visible coke deposition occurred.

It is known that Al–O bonds in the zeolite framework can be easily attacked by the HCl formed during reaction leading to the formation of volatile $AlCl_3$ (boiling point, 178°C) which causes the partial collapse of the framework and the blockage of the porous structure [32,55,56]. The degree of dealumination depends on the structure of the zeolite, the reaction temperature, and is strongly favoured in the presence of water [57]. Chlorine balances closed above 85% up to 500°C under dry conditions. Nevertheless, a decrease to 75 from 85% was noted for H-Y and H-MOR samples at 550°C which indicated that the destructive interaction between the zeolite and hydrogen chloride started at this temperature. On the other hand, when water was added to the feed stream, chlorine balances were in the 65–80% range above 450°C. Therefore, catalyst degradation was anticipated and enhanced under humid conditions.

XRD patterns of the used samples were analysed in order to study the resistance of the zeolites to dealumination which results in a loss of cristallinity. Relative cristallinity was calculated based on changes in peak heights from XRD data. The cristallinity of deactivated H-Y and H-MOR zeolites declined to 80 and 90%, respectively, whereas no significant loss in cristallinity was found in H-ZSM-5 zeolite sample. A slight decrease in cristallinity was noticed in

all the deactivated samples under humid conditions with respect to those measured in the samples of the dry experiments. Therefore, H-ZSM-5 appeared to be more resistant to dealumination than H-MOR and H-Y. This can be related to the low aluminium content in H-ZSM-5 zeolite in comparison to aluminium-rich zeolites, thus indicating zeolites with high Si/Al ratios are stable catalysts to oxidise CVOCs.

4. Conclusions

The oxidative decomposition of DCE over H-Y, H-ZSM-5 and H-MOR zeolite catalysts has been experimentally studied under dry and humid conditions. H-type zeolites tested in this study are reported to be effective in the catalytic destruction of DCE at temperatures ranging from 200 to 550°C. The conversion trend resulted the following: H-ZSM-5 > H-MOR > H-Y. TPD of ammonia and diffuse reflectance FT-IR measurements of adsorbed pyridine revealed that strong Brønsted acidity plays an important role in controlling the oxidative activity of the H-type zeolites. In addition, DRIFTS experiments indicated that DCE was primarily adsorbed on H-ZSM-5 zeolite through interaction with Brønsted sites.

The oxidation of DCE was fairly rapid and occurred at relatively low temperatures. However, this fast decomposition is accompanied by the generation of vinyl chloride as an intermediate which required higher temperatures for complete oxidation to CO, CO_2 and HCl. As far as CO and CO_2 formation was concerned, H-Y and H-MOR appeared to be more selective to CO_2 than H-ZSM-5. However, large amounts of carbon monoxide were measured over the three zeolites reflecting the difficulty of its oxidation using these catalysts. On the contrary, when vinyl chloride was decomposed, H-type zeolites showed a high selectivity (>90%) towards the desired chlorinated deep oxidation product, i.e. HCl.

The presence of water in the feed stream did not alter the order of activity observed in the dry experiments. The activity of the zeolites was reduced under humid conditions. Moreover, the presence of water in the DCE decomposition changed significantly the reaction product distribution. Vinyl chloride formation was found to be significantly reduced over the three zeolites. In addition, CO_2 selectivity was largely enhanced. XRD analysis of the deactivated samples indicated partial destruction of the zeolite crystal structure during reaction.

H-ZSM-5 results a suitable catalyst for CVOC destruction, because it offers good accessibility to active sites, high strong Brønsted sites concentration, great resistance to dealumination, and hydrophobic nature.

Acknowledgements

The authors wish to thank Universidad del País Vasco/EHU (UPV069.310-G40/98) and Ministerio de Educación y Cultura (QUI96-0471) for the financial support, and Gobierno Vasco for the Researchers Mobility Grant for one of the authors (P.S.). R. L.-F. acknowledges Ministerio de Educación y Cultura for the FPI grant.

References

[1] H. Muller, B. Deller, B. Despeyroux, E. Peldszud, P. Kammerhofer, W. Kuhn, R. Spielmannleitner, M. Stoger, Catal. Today 17 (1993) 383.
[2] A.R. Gavaskar, B.C. Kim, S.H. Rodansky, S.K. Ong, E.G. Marchand, Environ. Prog. 14 (1995) 33.
[3] M. Kosusko, M.E. Mullins, K. Ramanathan, T.N. Rogers, Environ. Prog. 7 (1988) 136.
[4] B. Mendyka, A. Musialik-Piotrowska, K. Syczewska, Catal. Today 11 (1992) 610.
[5] J.J. Spivey, J.B. Butt, Catal. Today 11 (1992) 465.
[6] L. Storaro, R. Ganzerla, M. Lenarda, R. Zanoni, A. Jiménez-López, P. Olivera-Pastor, E. Rodríguez-Castellón, J. Mol. Catal. A 115 (1997) 329.
[7] R.M. Lago, M.L.H. Green, S.C. Tsang, M. Odlyha, Appl. Catal. B 8 (1996) 107.
[8] R. Schneider, D. Kiessling, G. Wendt, W. Burckhardt, G. Winterstein, Catal. Today 47 (1999) 429.
[9] S. Kawi, M. Te, Catal. Today 44 (1998) 101.
[10] N.Y. Chen, T.F. Degnan, Chem. Eng. Prog. (1998) 32.
[11] A. Corma, A. Martínez, Catal. Rev. Sci. Eng. 35 (1993) 483.
[12] D.M. Ruthven, Chem. Eng. Prog. (1988) 43.
[13] S. Imamura, H. Tarumoto, S. Ishida, Ind. Eng. Chem. Res. 28 (1989) 1449.
[14] S. Chatterjee, H.L. Greene, J. Catal. 130 (1991) 76.
[15] S. Karmakar, H. L Greene, J. Catal. 138 (1992) 364.
[16] C.M. Schillmoller, Chem. Eng. 39 (1980) 161.
[17] Guía para la valoración de la contaminación del aire, in: Colección Senda Ambiental, Vol. 2, Ministerio de Sanidad y Consumo, Madrid, 1985 (in Spanish).
[18] A.E. Greenberg, L.S. Clesceri, A.D. Eaton (Eds.), Standard Methods for the Examination of Water and Wastewater, 18th Edition, American Public Health Association, Washington, 1992, p. 4.43.

[19] G. Marcelin, Catalysis 10 (1993) 83.
[20] T. Barzetti, E. Salli, D. Moscotti, L. Forni, J. Chem. Soc., Faraday Trans. 92 (1996) 1401.
[21] B. Chakraborthy, B. Viswanathan, Catal. Today 49 (1999) 253.
[22] J.A. Lercher, C. Gründling, G. Eder-Mirth, Catal. Today 27 (1996) 253.
[23] G. Busca, Catal. Today 41 (1998) 191.
[24] A. Auroux, J. Datka, Appl. Catal. A 165 (1997) 473.
[25] R.S. Drago, S.C. Dias, M. Torrealba, L. de Lima, J. Am. Chem. Soc. 119 (1997) 4444.
[26] C.V. Hidalgo, H. Itoh, T. Hattori, M. Niwa, Y. Murakami, J. Catal. 85 (1984) 362.
[27] S.B. Sharma, B.L. Meyers, D.T. Chen, J. Miller, J.A. Dumesic, Appl. Catal. A 102 (1993) 253.
[28] M. Maache, A. Janin, J.C. Lavalley, E. Benazzi, Zeolites 15 (1995) 507.
[29] A. Alberti, Zeolites 19 (1997) 411.
[30] D. Kiebling, R. Schneider, P. Kraak, M. Haftendorn, G. Wendt, Appl. Catal. B 19 (1998) 143.
[31] H. Nagata, T. Takakura, S. Tashiro, M. Kishida, K. Mizuno, I. Tamori, K. Wakabayashi, Appl. Catal. B 5 (1994) 23.
[32] M. Tajima, M. Niwa, Y. Fujii, Y. Koinuma, R. Aizawa, S. Kushiyama, S. Kobayashi, K. Mizuno, H. Ohûchi, Appl. Catal. B 9 (1996) 167.
[33] H. Greene, D. Prakash, K. Athota, G. Atwood, C. Vogel, Catal. Today 27 (1996) 289.
[34] J.R. González-Velasco, R. López-Fonseca, A. Aranzabal, J.I. Gutiérrez-Ortiz, P. Steltenpohl, Appl. Catal. B 24 (2000) 233.
[35] S. Chatterjee, H.L. Greene, Y. Joon Park, J. Catal. 138 (1992) 179.
[36] R. Buzzoni, S. Bordiga, G. Ricchiardi, C. Lamberti, A. Zecchina, G. Bellusi, Langmuir 12 (1996) 930.
[37] M. Guisnet, P. Magnoux, Appl. Catal. 54 (1989) 1.
[38] K. Ramanathan, J.J. Spivey, Combust. Sci. Technol. 47 (1986) 229.
[39] H. Windawi, M. Wyatt, Platinum Metals Rev. 37 (1993) 186.
[40] J.R. González-Velasco, A. Aranzabal, J.I. Gutiérrez-Ortiz, R. López-Fonseca, M.A. Gutiérrez-Ortiz, Appl. Catal. B 19 (1998) 189.
[41] J. Weldon, S.M. Senkan, Combust. Sci. Technol. 47 (1986) 229.
[42] G. Laidig, D. Honicke, K. Griesbaun, Erdor. Kohle-Ergas-Petrochem. 34 (1981) 329.
[43] J.C. Lou, S.S. Lee, Appl. Catal. B 12 (1997) 111.
[44] X.-Z. Jiang, L.-Q. Zhang, X.-H. Wu, L. Zheng, Appl. Catal. B 9 (1996) 229.
[45] R.W. van der Brink, P. Mulder, R. Louw, G. Sinquin, C. Petit, J.-P. Hindermann, J. Catal. 180 (1998) 153.
[46] R.W. van der Brink, R. Louw, P. Mulder, Appl. Catal. B 16 (1998) 219.
[47] J.A. Rossin, M.M. Farris, Ind. Eng. Chem. Res. 32 (1993) 1024.
[48] J.M. Freidel, A.C. Frost, K.J. Herbert, F.J. Meyer, J.C. Summers, Catal. Today 17 (1993) 367.
[49] B. Ramachandran, H.L. Greene, S. Chatterjee, Appl. Catal. B 8 (1996) 157.
[50] J.A. Rabo, G.J. Gajda, Catal. Rev. Sci. Eng. 31 (1990) 385.
[51] D.S. Prakash, K.V. Athota, H.L. Greene, C.A. Vogel, AIChE Symp. Ser. 91 (1995) 1.
[52] J.R. González-Velasco, A. Aranzabal, R. López-Fonseca, R. Ferret, J.A. González-Marcos, Appl. Catal. B 24 (2000) 33.
[53] S. Chatterjee, H.L. Greene, Y.J. Park, Catal. Today 11 (1992) 569.
[54] L. Becker, U. Hatje, H. Forster, Stud. Surf. Sci. Catal. 94 (1995) 627.
[55] S. Karmakar, H.L. Greene, J. Catal. 148 (1994) 524.
[56] M. Briend-Faure, O. Cornu, D. Delafosse, R. Monque, M.J. Pelter, Appl. Catal. 38 (1988) 71.
[57] Z. Konya, I. Hannus, I. Kiricsi, Appl. Catal. B 8 (1996) 391.